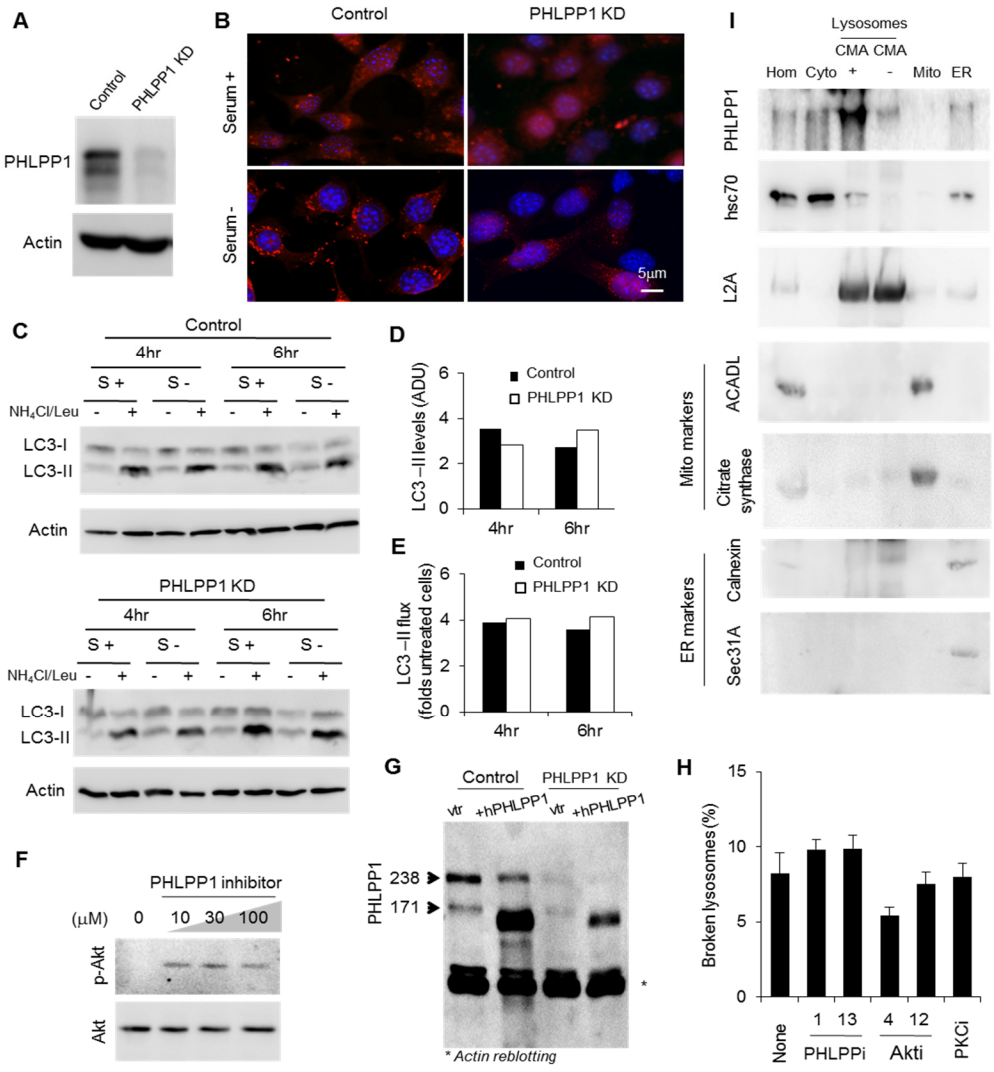

Figure S1. PHLPP1 knock-down and autophagy, related to Fig. 1 and 2. (**A**) Immunoblot for PHLPP1 of mouse fibroblasts stably transduced with an empty lentiviral vector (Control; Ctr) or lentivirus carrying shRNA against PHLPP1 (KD). (**B**) Representative images of the same cells stably expressing KFERQ-PA-mCherry1 maintained in the presence or absence of serum. These images are wide fields in color of the higher magnification images shown in Fig. 1A. (**C**) Immunoblot for LC3-II in mouse fibroblasts control (top) or KD for PHLPP1 (bottom) cultured in the presence (+) or absence (-) of serum for the indicated periods of time and treated (+) or not (-) with lysosomal inhibitors ammonium chloride and leupeptin. (**D, E**) Steady-state LC3-II levels (**D**) and LC3-II flux (**E**) calculated as described under experimental procedures by the densitometric quantification of the immunoblot shown in C. (**F**) Immunoblot for phosphorylated and total Akt in cells maintained in the absence of serum supplemented with increasing concentrations of a PHLPP1 inhibitor as indicated. (**G**) Immunoblot for PHLPP1 in mouse fibroblasts control (Ctr) or knock-down (KD) for PHLPP1 transfected with an empty vector (vtr) or a plasmid coding for human full length PHLPP1 (+hPHLPP1). The same membrane was reblotted for actin as a loading control. (**H**) Hexosaminidase activity detected in the incubation media of freshly isolated lysosomes incubated with the indicated inhibitors of PHLPP1, Akt and PKC. The percentage of broken lysosomes was calculated as the percentage of total hexosaminidase activity in lysosomes detected in the incubation media. Values are mean+s.e.m. n= 3. (**I**) Immunoblot in mouse cellular fractions for protein markers of different cellular compartments. Hom: homogenate; Cyto: cytosol; CMA+ and CMA-: lysosomes active or not for CMA, respectively; Mito: mitochondria; ER: endoplasmic reticulum.

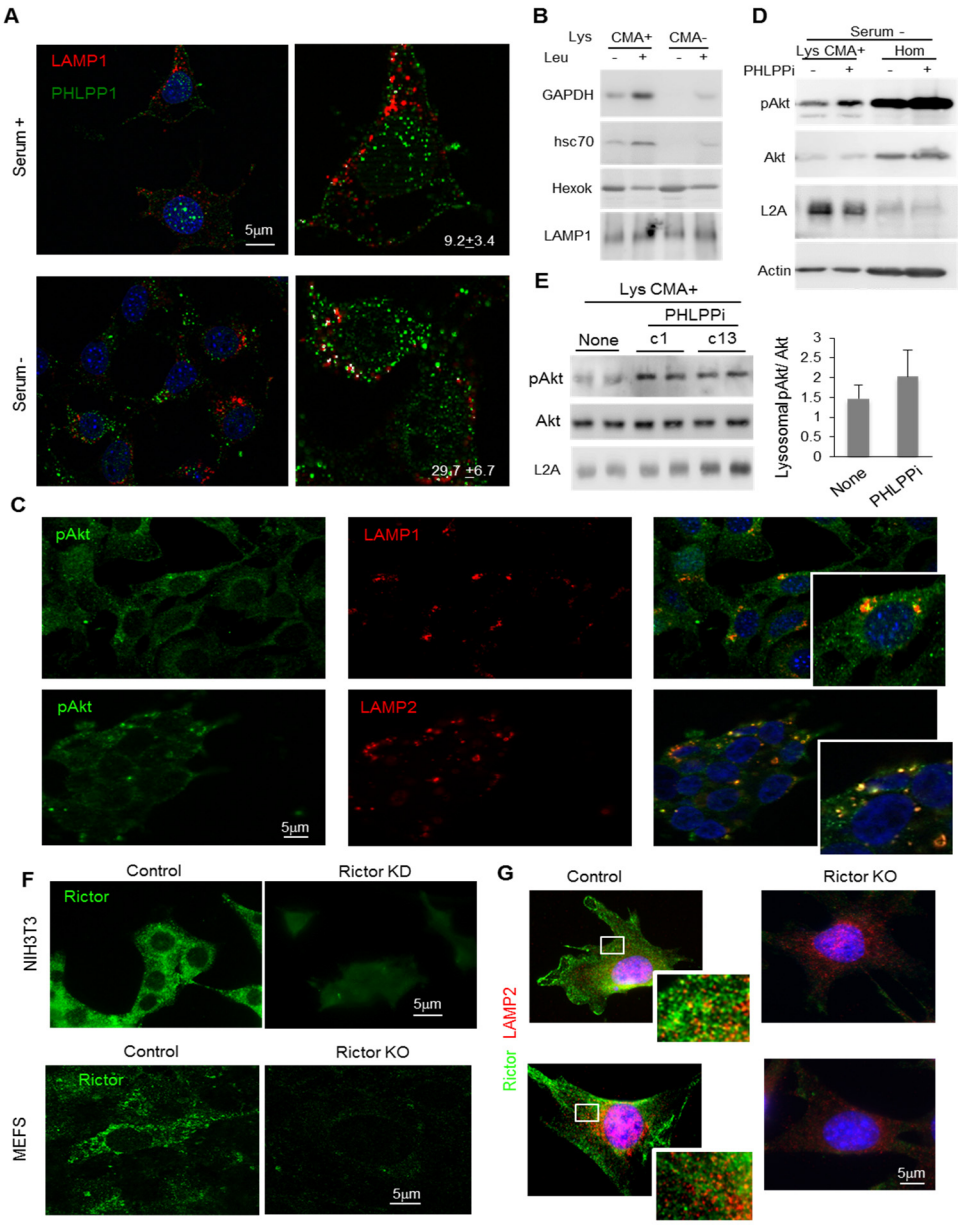

Figure S2. Lysosomal association of CMA regulatory kinases and phosphatases, related to Fig. 2 and 3. (**A**) Representative images of the co-immunostaining for LAMP1 and PHLPP1 in mouse fibroblasts maintained in serum supplemented (+) or depleted (-) media for 24h. Right panels show higher magnification and colocalization pixels in white. Nuclei were highlighted with DAPI. Percentage of colocalization is indicated. (**B**) Immunoblot of CMA active (+) and inactive (-) lysosomes (Lys) isolated from rats untreated (-) or injected with leupeptin 2h before isolation (+). Levels of a well-characterized CMA substrate (GAPDH) and a CMA non-substrate (Hexokinase) are shown. (**C**) Co-immunostaining for pAkt and LAMP1 or LAMP2 in mouse fibroblasts maintained in serum-supplemented media. Single and merged channels are shown. (**F**) Immunoblot for the indicated proteins of lysosomes isolated from cells maintained in the absence of serum for 24h and treated or not with the PHLPP1 inhibitor, as labeled. Independent experiment to the one shown in Fig. 3F to support reproducibility of the lysosomal pAkt changes. (**G**) Immunoblot for the indicated proteins in starved rat liver lysosomes active for CMA treated with the indicated PHLPP inhibitors. Right: Quantification of the ratio of phosphorylated Akt (pAkt) to unmodified Akt in lysosomes upon addition of the inhibitors. n=6. Values are mean+s.e.m. (**F**) Immunostaining for Rictor in mouse fibroblasts control or knock down for Rictor and in MEFS from control and rictor knock-out mice. (**G**) Co-immunostaining for Rictor and LAMP2 in mouse embryonic fibroblasts control or knock out for Rictor. Inset shows higher magnification of the boxed area.

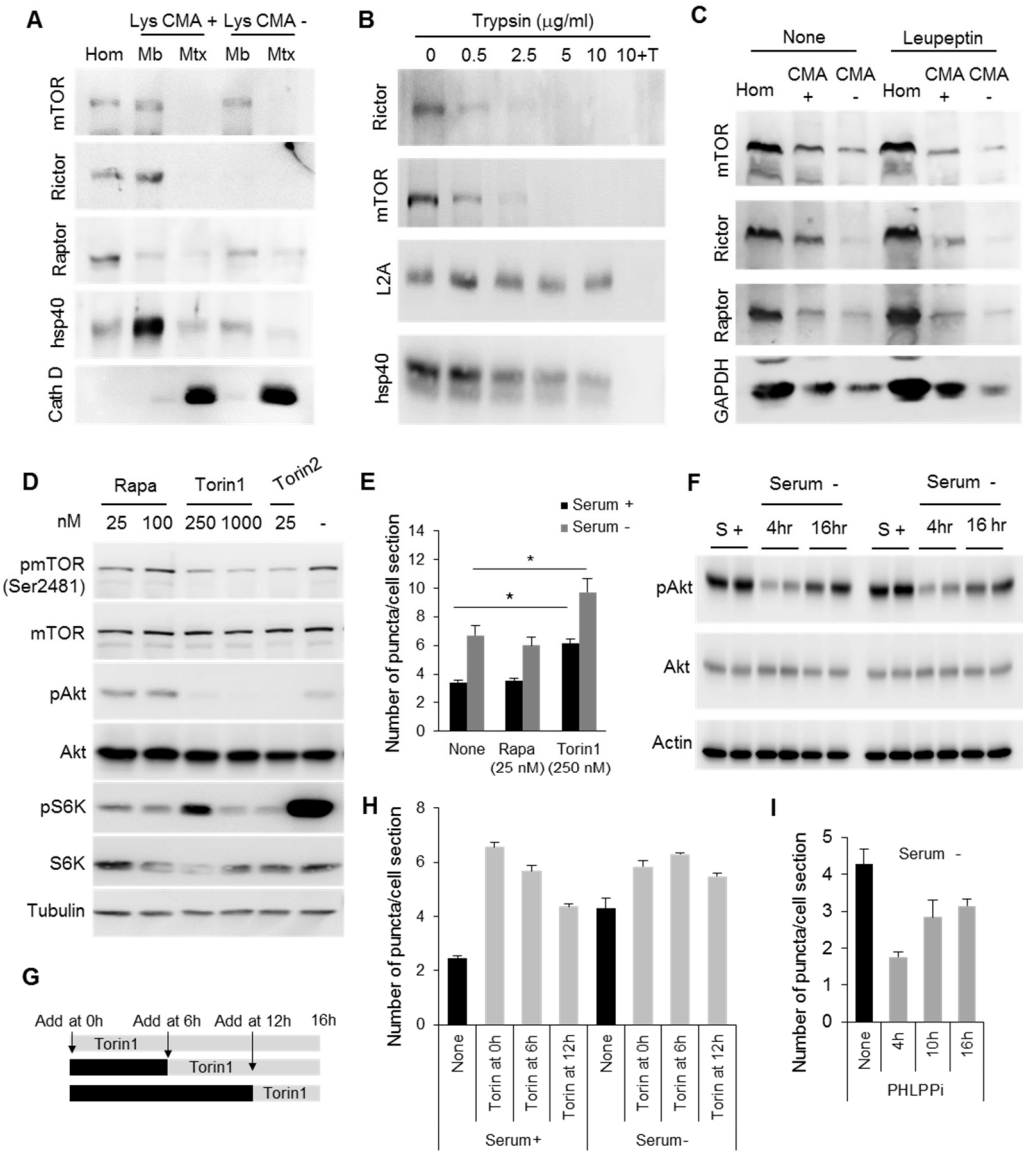

Figure S3. Lysosomal topology of TORC2 and regulatory effect of the TORC2-Akt-PHLPP1 axis on CMA, related to Fig. 3 and 4. (**A**) Immunoblot of homogenates (Hom) and membranes (Mb) and matrices (Mtx) of lysosomes with high (+) or low (-) CMA activity isolated from starved rat liver. (**B**) Immunoblot of intact lysosomes treated with increasing concentrations of trypsin alone or with Triton X-100 (T). (**C**) Immunoblot of lysosomes with high (+) or low (-) CMA activity isolated from starved rats untreated (None) or injected with leupeptin 2h before isolation. (**D**)**.** Immunoblot for the indicated proteins in mouse fibroblasts treated as labeled. (**E**) Quantification of changes in CMA activity in fibroblasts stably expressing KFERQ-PA-mCherry1 and subjected to the indicated treatments. Quantification was performed in n >75 cells. Representative images are shown in Fig. 4A. (**F**) Immunoblot to monitor changes in the phosphorylation status of Akt in cells maintained in serum supplemented or serum deprived media for the indicated periods of time. Two independent experiments run in the same blot are shown. (**G**) Diagram of the time course to check the effect of Torin1 on CMA activity. Cells were maintained in serum-supplemented or serum-deprived media as indicated, and Torin1 was added from the beginning (Time 0) or 6 or 12h later; all cells were fixed 16h after changing the media. (**H**) Graph showing results measured in cells expressing KFERQ-PS-Dentra2 CMA reporter as the average number of puncta per cell; quantification was performed by high-content microscopy in n>850 cells. (**I**) Effect of PHLPP inhibitor added to cells maintained in serum-deprived media following a similar scheme as the one described in H. Quantification was performed as in H.

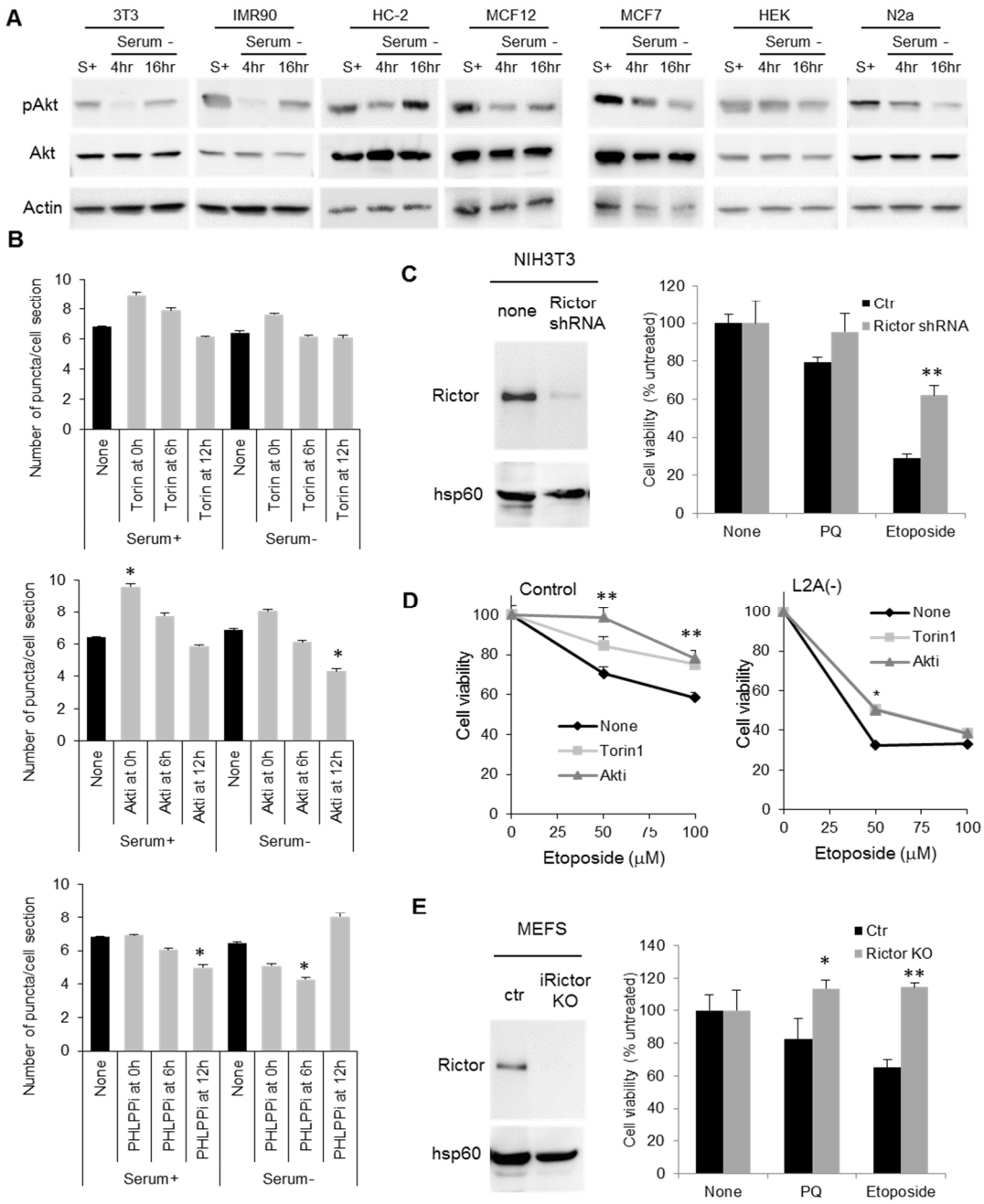

Figure S4. Regulatory effect of the TORC2-Akt-PHLPP1 axis on CMA in different cell types and physiological relevance of this regulatory axis in the response to stressors, related to Fig. 4 and 5. (**A**) Immunoblot of total cell lysate isolated from different cell lines maintained in the presence of serum (S+) or at the indicated times upon serum removal. (**B**) Effect of Torin1, Akt inhibitor or PHLPP inhibitor added following a similar scheme to the one shown in Fig. S3H but to mouse neuroblastoma cells N2a transduced with the KFEQR-Dendra2 reporter. Quantification was performed as in Fig. S3H. (**C**) Immunoblot to confirm Rictor knockdown efficiency (*left*) and cellular viability in response to the indicated stressors. n=6. (**D**) Viability of cells control or knocked down for LAMP-2A (L2A(-)) subjected to increasing concentrations of etoposide without additional treatment (None) or in the presence of Torin1 (250nM) or Akt inhibitor (3μM). n=3. (**E**) Immunoblot to confirm Rictor knockout efficiency (*left*) and cellular viability in response to the indicated stressors. n=6. All values are mean+s.e.m., and differences are significant for *p<0.05 or **p<0.01.

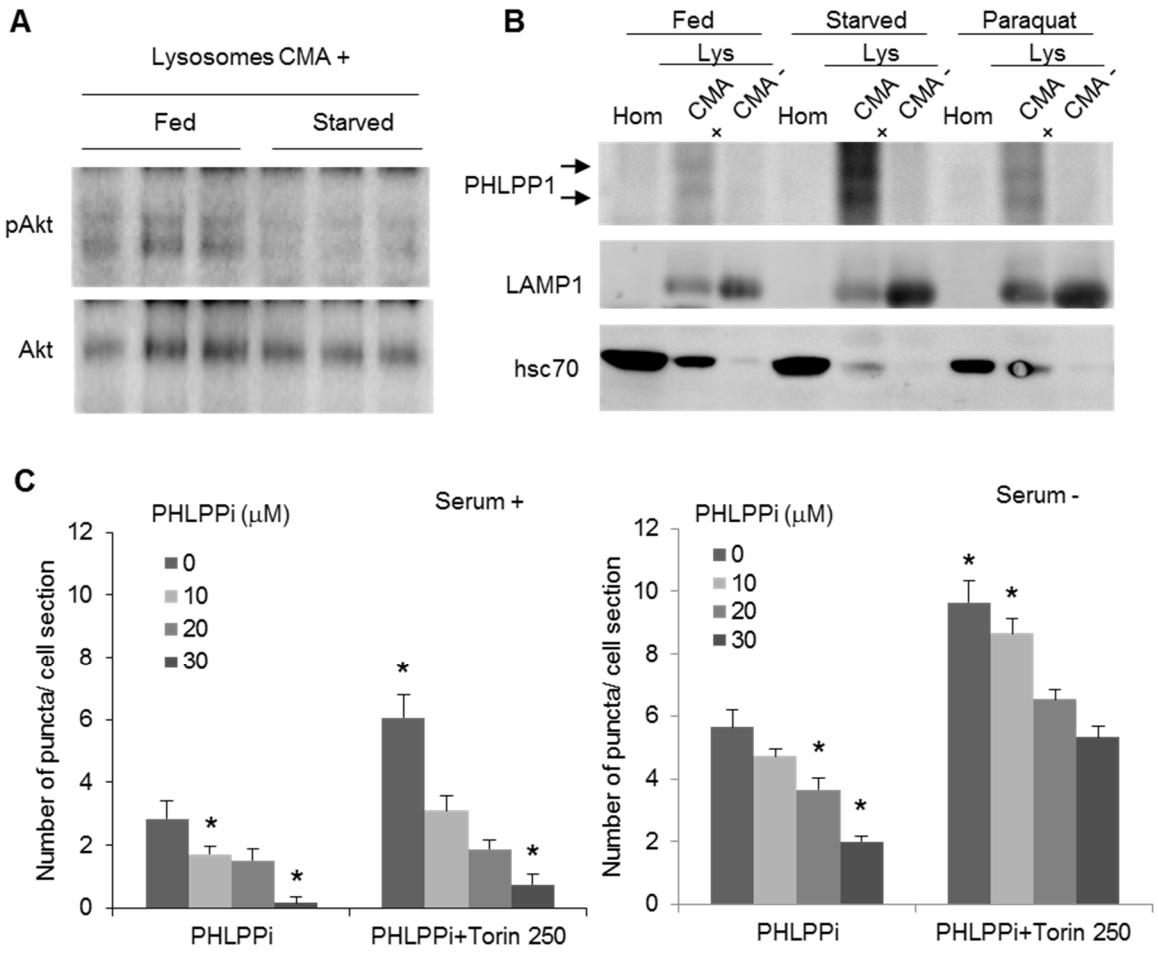

Figure S5. Stress-induced changes in lysosomal levels and activity of PHLPP and pAkt, related to Fig. 5. (**A**) Immunoblot for PHLPP1 of homogenates (Hom) and lysosomes with high (+) and low (-) CMA activity isolated from livers of rats normally fed, starved for 48h or subjected to two injections of paraquat separated by 24h to induce mild oxidative stress. Levels of hsc70 are shown as proof of separation of both types of lysosomes. (**B**) Immunoblot for total and phosphorylated Akt in lysosomes active for CMA isolated from livers of normally fed or 48h starved rats. (**C**) Quantification by high-content microscopy (HCM) of the changes in CMA activity (average number of puncta per cell section) in mouse fibroblasts expressing KFERQ-PS-Dendra2 CMA reporter maintained in the presence or absence of serum and treated with the indicated concentrations of PHLPP inhibitor (PHLPPi) alone or in the presence of 250nM Torin1. Values are mean+s.e.m.. n>800 cells and differences with untreated cells are significant for $p<0.05$.

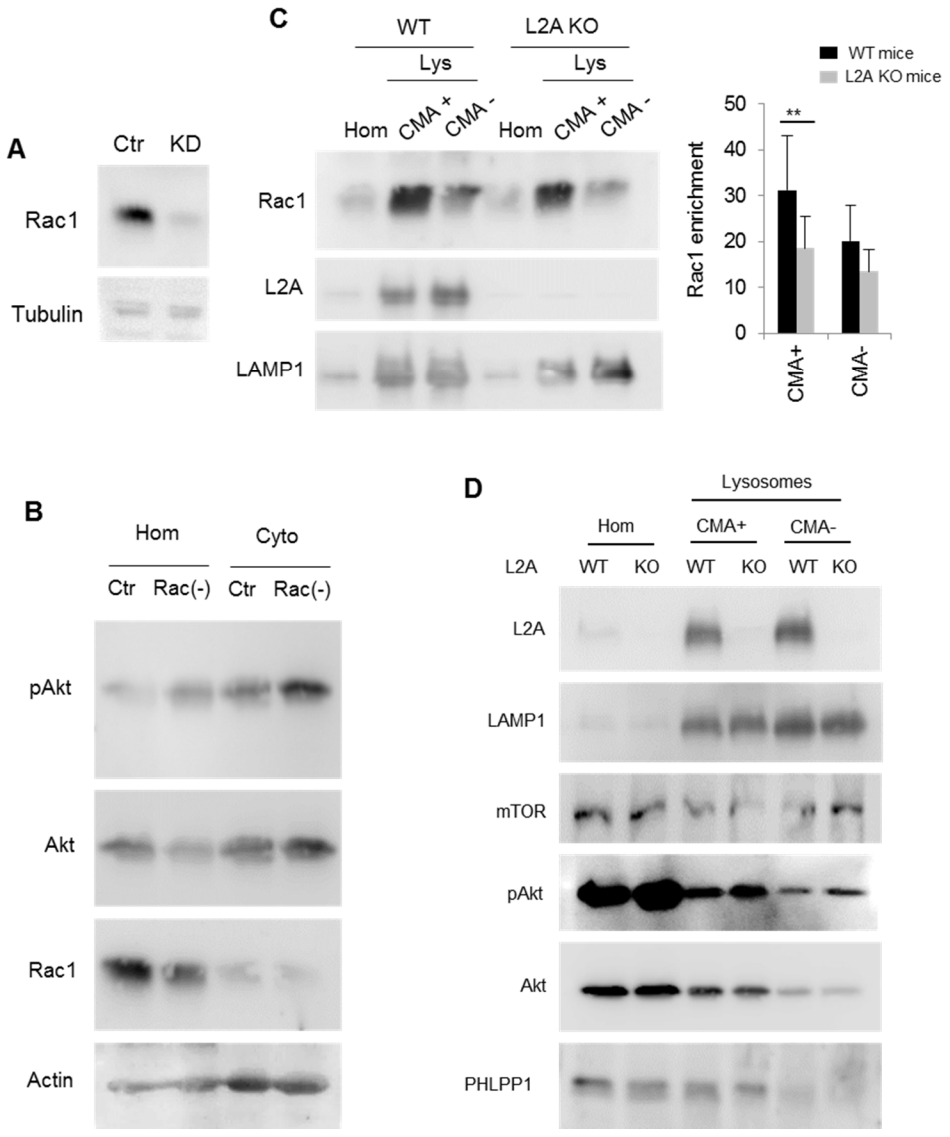

Figure S6. **Efficiency of Rac-1 knock-down and changes in components of the mTORC2/PHLPP1/AKT axis and Rac1 in a LAMP-2A deficient mouse model, related to Fig. 6.** (**A**) Immunoblot in cells control (Ctr) or knock-down for Rac1. (**B**) Immunoblot of homogenate (Hom) and cytosol (Cyto) from cells control (Ctr) or knock-down for Rac1 (Rac (-)) maintained in serum-deprived media for 24h. (**C, D**) Immunoblot of homogenates (Hom) and lysosomes active (+) or inactive (-) for CMA isolated from livers of wild-type mice (WT) or liver-specific LAMP-2A knock-out mice (Alb-Cre-L2A KO). Quantification on the right in C, shows lysosomal enrichment of Rac1. Values are mean+s.e.m. n=3. Differences with control cells are significant for $p<0.05$.

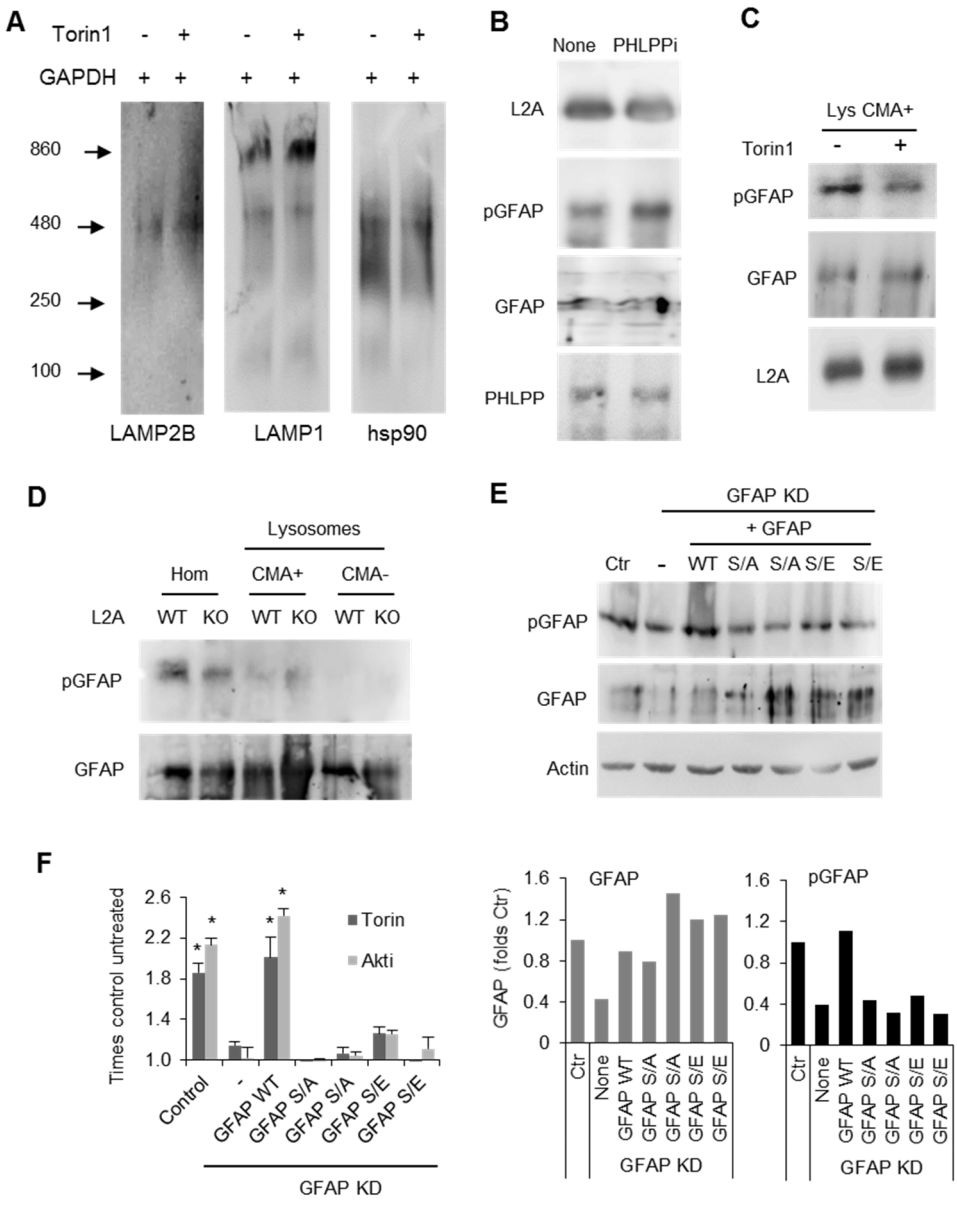

Figure S7. **Effect of the mTORC2/PHLPP1/Akt axis on the multimeric status of lysosomal proteins and phosphorylation of GFAP, related to Fig. 7. (A)** Effect of Torin1 on the multimeric state of lysosomal proteins. (**B, C**) Immunoblot of lysosomes isolated from starved (**B**) and fed (**C**) rats upon treatment with the indicated inhibitors. (**D**) Immunoblot of homogenates (Hom) and lysosomes active (+) or inactive (-) for CMA isolated from livers of wild-type mice (WT) or liver-specific LAMP-2A knock-out mice (Alb-Cre-L2A KO). Controls are shown in S6E as these immunoblots are reblotting of those membranes. (**E**) Mouse fibroblasts control (Ctr) or knock-down for GFAP untransfected (-) or transfected with plasmids carrying GFAP in which the S in the putative Akt phosphorylation site has been mutated to A, or to E to mimic constitutive phosphorylation. Graphs at the bottom show levels of total GFAP and phosphorylated GFAP. (**F**) Effect of Torin1 and Akt inhibitor on the CMA activity of cells shown in E. Values are expressed as folds CMA activity in their respective untreated controls. Values are mean+s.e.m. n=6. Differences with untreated cells are significant for $p<0.05$.

Supplemental Experimental Procedures

Cell lines

NIH3T3 mouse fibroblasts, the mouse neuroblastoma cell line (N2a), non-tumorigenic (MCF12) and cancer (MCF7) human breast epithelial cell lines and human cardiac muscle cells (H9C2) were from the American Type Culture Collection; human lung fibroblasts IMR-90 were from the Coriell Cell Repository, human embryonic kidney 293 cells (HEK293) from the NCI repository and mouse embryonic fibroblasts (MEF) from wild type (WT), Akt1-/- (1KO) and Akt2-/- (2KO) mice were a gift from Dr. Birnbaum (University of Pennsylvania) (Bae et al., 2003). The Inducible rictor knockout mouse embryonic fibroblasts were a gift from Dr. Michael N. Hall (Cybulski et al., 2012). Cells stably knocked down for PHLPP1, rictor, GFAP or Rac1 were generated as described previously (Massey et al., 2006) using the following lentiviral-delivered small hairpin RNA (shRNA) from the Mission-Sigma library (Sigma-Aldrich) against PHLPP1 (TRCN0000081362), GFAP (TRCN0000090603), rictor (TRCN0000123395) and Rac1 (TRCN0000055188). Cells were maintained in Dulbecco's modified Eagle's medium (DMEM) (Sigma, St. Louis, MO), or high glucose DMEM (Hyclone, St. Louis, MO) in the presence of 10% newborn calf serum (NCS) or 10% fetal bovine serum (FBS).

Chemicals and plasmids

The inhibitors of Akt were from EMD MILLIPORE, of PHLPP1 from the National Cancer Institute (NCI IDs; NSC 117079), and of Protein kinase C (PKC) from Promega (V5691). Rapamycin was from Calbiochem and Torin1 and Torin2 were from Tocris. Methyl viologen dichloride hydrate (Paraquat), Thapsigargin and Etoposide were from Sigma-Aldrich. The antibodies against mouse LAMP1 (1D4B) and human LAMP2 (H4B4) were from the Developmental Hybridoma Bank (University of Iowa), against mouse LAMP-2A from Invitrogen, against rat LAMP1, actin, hsp40 and hsp90 from Stressgen, against GAPDH from Abcam, against α-synuclein from BD Transduction Laboratories, against tubulin from Sigma, against light chain 3 protein (LC3), Akt, pAkt (Ser473), mTOR, pmTOR (Ser2481), Rictor, Raptor, pS6K, S6K, RagB, RagD, Rheb, Acyl-CoA dehydrogenase, Citrate synthase, Calnexin and Sec31 from Cell Signaling, against

Cathepsin D and Rictor from Santa Cruz, against Rac1 and GFAP from Millipore and against pGFAP from Abgent, against hsc70 was from Novus. The antibody against PHLPP1 was from Bethyl. The polyclonal antibody against the cytosolic tail of LAMP-2B was developed in our laboratory (Massey et al., 2006). Primers to mutate S in GFAP either to A or E respectively were as follow: Direct 5' GGAGAGGAGACGCAGCACCTCCGCTGCTCGCCGCTCC 3´; Rev 5' GGAGCGGCGAGCAGCGGAGGTGCTGCGTCTCCTCTCC 3'; Direct 5' GGAGAGGAGAC GCAGAACCTCCGCTGCTCGCCGCTCC 3'; Rev 5' GGAGCGGCGAGCAGCGGAGGTTC TGCGTCTCCTCTC C 3'.

Measurement of CMA activity

To measure CMA in isolated lysosomes they were incubated with a pool of [^{3}H]-labeled cytosolic proteins in 3-(N-morpholino)propanesulfonic acid (MOPS) buffer (10mM MOPS, pH 7.3, 0.3M sucrose, 1mM dithiothreitol, and 5.4μM cysteine) for 20min at 37^{o}C and after precipitation in acid, proteolysis was calculated as the acid precipitable radioactivity (protein) transformed to acid soluble (amino acid). In a second assay, lysosomes were incubated with purified proteins, subjected to immunoblot and binding and uptake calculated.

To measure *CMA activity in intact cells* the photoactivable (PA) KFERQ-PA-mCherry1 and photoswitchable KFERQ-PS-CFP were used for conventional microscopy and the KFERQ-PS-Dendra2 for high-content microscopy. Cells were photoactivated with a 405nm light emitting diode (LED: Norlux) for 4min with the intensity of 3.5mA (current constant). Cells were fixed with 4% paraformaldehyde and images were acquired with an Axiovert 200 fluorescence microscope (Carl Zeiss Ltd.), with1.4 numerical aperture and ApoTome.2 slider. The number of fluorescent puncta by cell was quantified using Image J (NIH) in individual single planar images after thresholding. For high-content microscopy in 96-well plates images were captured with a high-content microscope (Operetta system, Perkin Elmer) and quantification was performed with the manufacturer's software in a minimum of 800 cells (approx. 9 fields). In all cases, focal plane thickness was set at 0.17 μm and sections with maximal nucleus diameter were selected for

quantification. Values are presented as number of puncta per cell section that in our acquisition conditions represents 10-20% of the total puncta per cell.

Electrophoresis and immunoprecipitation procedures

Electrophoresis and immunoblot were performed using nitrocellulose membranes after cell lysis in RIPA buffer (1% Triton-X 100, 1% sodium deoxycholate, 0.1% SDS, 0.15M NaCl, 0.01M sodium phosphate, pH 7.2) containing protease and phosphatase inhibitors. The proteins of interest were visualized by chemiluminescence using peroxidase-conjugated secondary antibodies in LAS-3000 Imaging System (Fujifilm). *Blue native electrophoresis* was performed in 1% octylglucoside-solubilized samples mixed with sample buffer for Blue Native Page (Life Technologies).

Protein co-immunoprecipitation was performed by incubation with primary antibodies and sepharose-immobilized protein A/C of samples solubilized in 25mM Tris (pH 7.2), 150mM NaCl, 5mM $MgCl_2$, 0.5% NP-40, 1mM DTT, 5% glycerol. For the phosphorylation assays, Akt was immunoprecipitated with immobilized pAkt (Ser473) antibody in 40mM HEPES, 2mM EDTA, 10mM pyrophosphate, 10mM glycerol phosphate, 0.3% CHAPS and incubated with purified GFAP in the recommended kinase buffer for 30min at 30°C.

Supplemental References

Bae, S.S., Cho, H., Mu, J., and Birnbaum, M.J. (2003). Isoform-specific regulation of insulin-dependent glucose uptake by Akt/protein kinase B. J Biol Chem *278*, 49530-49536.

Cybulski, N., Zinzalla, V., and Hall, M.N. (2012). Inducible raptor and rictor knockout mouse embryonic fibroblasts. Methods Mol Biol *821*, 267-278.

Massey, A.C., Kaushik, S., Sovak, G., Kiffin, R., and Cuervo, A.M. (2006). Consequences of the selective blockage of chaperone-mediated autophagy. Proc Nat Acad Sci USA *103*, 5905-5910.